Greg Wilson graduated Summa Cum Laude from California State University, Hayward, earning a BS degree in mathematics in 1977. In 1979, he graduated with an MS degree in mathematics from the same institution with highest honors, while maintaining a 4.0 GPA. In 1983, he received his PhD in mathematics from the University of California at Santa Barbara, working in the field of modular function theory. Since joining Mission Research in 1983, Dr. Wilson has been exposed to a wide variety of physics and engineering problems. As a result, he has developed several areas of interest resulting in well over 30 reports or publications in diverse areas, including one voted best technical paper for the AMTA symposium of 2001/2002.

Kramers-Kronig Analysis of RF Polymers and Composites

Mark M. Scott, Gregory L. Wilson, and Jeffery A. Berrie

ATK–Mission Research Corporation
Dayton, Ohio 45430, USA

Abstract

A piecewise-linear model of the Kramers-Krönig (K-K) relations has been used to analyze electromagnetic dispersion data on RF polymers and composites. This K-K analysis revealed that concrete knowledge about the complex low-frequency material dispersion is critical to the analysis and understanding of the microwave dispersion. Furthermore, and more practically, the confidence in the material dispersion measurements may be, to some degree, ascertained through use of the K-K relations.

Keywords: Permeability measurement; permittivity measurement; electromagnetic dispersion; nonhomogeneous media; dielectric materials; materials testing

1. Introduction

The measurement of the complex electromagnetic dispersion of materials is important for the design of various microwave structures. Although many techniques exist for the acquisition of a material's dispersion [1], the analysis of the extracted parameters that describe this dispersion (the complex permittivity and permeability) presents various challenges. Among these challenges, (1) the accuracy of extracted parameters is difficult to determine due to the lack of material standards; and (2) the extracted imaginary part of the material dispersion (dielectric or magnetic loss), for low loss materials, typically possesses large uncertainty.

One way to address these challenges is to use the Kramers-Krönig (K-K) relations [2-4], which relate the real and imaginary parts of the complex material dispersion over all frequencies, as a data-analysis tool. In this work, these relations were employed to analyze various complex permittivity data on RF polymers and magnetic polymer composites. The analysis performed during this work was general, and could be extended to various other complex material parameters (see, e.g., [5, 6] and references therein), including permeability.

The practical origin of this work arose from trends observed in microwave and RF dielectric measurements of composites engineered at ATK-Mission Research Corporation. The data on these magnetic ceramic and metal-loaded composites revealed two tendencies. First, and rather obviously, as the percent loading of relatively high-dielectric-constant ceramic or metal increased, the composite material's permittivity increased. Second, the increase in the material's permittivity was accompanied by an increase in the permittivity loss. These trends implied a connection between the permittivity and permittivity loss. In particular, the permittivity loss was shown to scale with the permittivity (this general trend was also observed between the permeability and permeability loss).

The team at Mission Research Corporation decided to explore the observed trend in the data with the K-K relations. The primary goal was to establish whether some type of fundamental limit on the loss existed, associated with an increase in the real part of the permittivity or permeability. Such a fundamental limit could prohibit the manufacture of useful composite materials with wave impedances greater than that of free space [7].

As a consequence of this K-K analysis, the observed trend was explained to some degree, and other interesting features were revealed. Section 2 presents a brief theoretical background discussion of materials and the K-K relations. Section 3 introduces and addresses the details of the piecewise-linear model used in conjunction with the K-K relations. Section 4 presents comparisons between the model and the data. Section 5 provides conclusions based on these comparisons.

2. Material Behavior and the Kramers-Krönig Relations

As a starting point to the implementation of the K-K relations, a background investigation into their origins was performed. A brief description of the K-K relations and their derivation will be given here, along with statements concerning their implications for materials. References [3], and especially [4], contain in-depth considerations of the K-K relations, and the discussion below draws from these texts.

When the frequency of an applied electric field varies *sufficiently rapidly*, the well-known relations

$$\mathbf{D} = \varepsilon \mathbf{E} \tag{1a}$$

and

$$\mathbf{B} = \mu \mathbf{H}, \tag{1b}$$

where ε and μ are *static*, *real* numbers, no longer hold. [As a point of reference, the free-space values of permittivity and permeability are $\varepsilon = \varepsilon_0 \approx 8.85 \times 10^{-12}$ F/m and $\mu = \mu_0 \approx 4\pi \times 10^{-7}$ H/m, respectively. These values are used to obtain the well-known impedance of free space: $Z_0 \approx \sqrt{\mu_0/\varepsilon_0} \approx 377\,\Omega$.] "Sufficiently rapidly" in the above context means that the frequency of the applied field oscillation is not small in comparison with the characteristic frequencies of the electric and magnetic polarizations of the concerned substance. As a consequence of these characteristic frequencies, the μ and ε of the materials are necessarily functions of the angular frequency, ω, of the applied field. They are now complex to account for material loss, that is, $\varepsilon \to \varepsilon'(\omega) - j\varepsilon''(\omega)$ and $\mu \to \mu'(\omega) + j\mu''(\omega)$. These expressions for the permittivity and the permeability are consistent with an $e^{+j\omega t}$ time convention, and should replace the constant values in Equations (1). Such a replacement yields

$$\mathbf{D}(\omega) = \varepsilon(\omega)\mathbf{E}(\omega) \tag{2a}$$

and

$$\mathbf{B}(\omega) = \mu(\omega)\mathbf{H}(\omega). \tag{2b}$$

These time-varying fields, characterized by ω, are necessarily variable in space, as well. Thus, at very large frequencies, the wavelength will be comparable to the material's atomic dimensions, and the macroscopic picture described by Equations (2) no longer holds. [The high-frequency limit for the permittivity, which arises due to the motion of bound, unpaired electrons, lies in the ultraviolet (UV) frequency band. Above UV frequencies, the real part of the relative permittivity is unity, and the permittivity loss is zero. As a further note, the high-frequency relative permeability limit for magnetic materials arises due to spin resonances, and lies in the low end of the microwave band. This is an unfortunate barrier for the fabrication of magnetic microwave/ RF polymer composites.] Furthermore, the connection implied between Equations (1) and (2) at very low frequencies suggests that at some finite frequency, Equations (2) do not differ appreciably from Equations (1). Thus, at sufficiently low frequencies (though still above dc), the concept of a frequency-dependent μ and ε is unnecessary. [The low-frequency limit for the permittivity, which arises due to electric dipolar resonances, lies below the UHF band. Below UHF, the ac permittivity does not differ significantly from the dc value.]

Nonetheless, there exists a range of frequencies (which include the RF/microwave region) where the macroscopic picture is valid *and* the dispersive character of the material (that is, the complex frequency-dependent permittivity and permeability) is important. It is in this region where the K-K relations, which connect the real and imaginary parts of the material dispersion through remarkably simple expressions, find great utility.

The key elements in the derivation of the K-K relations are: (1) the use of the Fourier integrals of **D** and **E**, (2) the consideration of the complex permittivity as a function of a complex variable $\omega \to \omega' - j\omega''$, (3) the determination of the analyticity of the complex permittivity, (4) the application of the Cauchy integral theorem [8], and (5) the statement of causality. Causality in this context means that the effect (the induced polarization in the material) cannot precede the cause (the applied electric field).

After the application of the above steps, the K-K relations obtained for $\varepsilon_r'(\omega) = \varepsilon'(\omega)/\varepsilon_0$ and $\varepsilon_r''(\omega) = \varepsilon''(\omega)/\varepsilon_0$ are typically first written in the form

$$\varepsilon_r'(\omega_0) = 1 + \frac{1}{\pi} P \int_{-\infty}^{\infty} \frac{\varepsilon_r''(\omega)}{(\omega - \omega_0)} d\omega,$$

$$\varepsilon_r''(\omega_0) = \frac{1}{\pi} P \int_{-\infty}^{\infty} \frac{\varepsilon_r'(\omega) - 1}{(\omega - \omega_0)} d\omega. \tag{3}$$

In Equations (3), P stands for the principal part of the complex integral [8], ω_0 is the constant angular frequency where the permittivity is evaluated, and ω is the angular frequency integration variable. The r subscripts in Equations (3) denote relative values, i.e., the real and imaginary parts of the permittivity have been normalized to the permittivity of free space, ε_0. Typically, Equations (3) are rewritten such that the integration covers only the range of positive frequencies. This is accomplished by exploiting the property $\varepsilon_r(-\omega) = \varepsilon_r^*(-\omega^*)$, which is a statement of the evenness and oddness of the real and imaginary parts of $\varepsilon_r(\omega)$ [2], respectively. The K-K relations then take the form

$$\varepsilon_r'(\omega_0) = 1 + \frac{2}{\pi} P \int_0^{\infty} \frac{\omega \varepsilon_r''(\omega)}{\omega^2 - \omega_0^2} d\omega \tag{4}$$

and

$$\varepsilon_r''(\omega_0) = -\frac{2\omega_0}{\pi} P \int_0^{\infty} \frac{(\varepsilon_r'(\omega) - 1)}{\omega^2 - \omega_0^2} d\omega. \tag{5}$$

Equations (4) and (5) are the commonly used versions of the K-K relations. These expressions show that the value of either component of the permittivity at *one* particular frequency ω_0 depends on the other component's behavior over *all* frequencies ω. As will be shown below, the scope of this dependence is remarkably far-reaching.

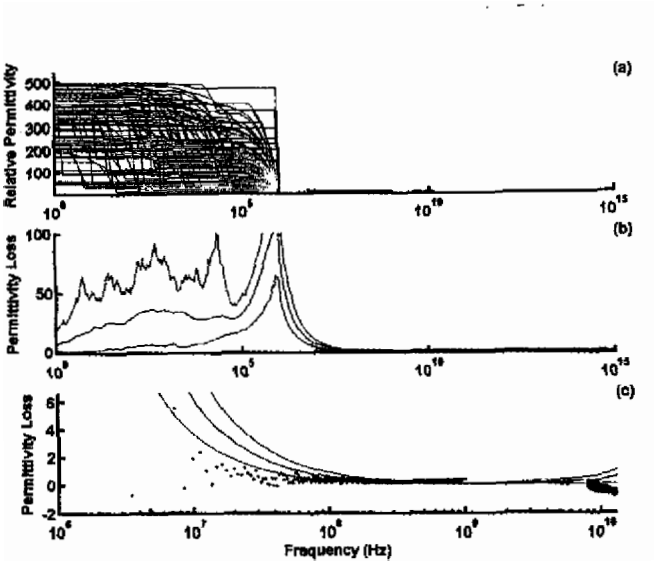

Figure 3. Plots of the real and imaginary parts of the relative permittivity as a function of frequency, overlaid on measured data. Graph (a) shows 100 realizations for the real part of the permittivity (red curves) along with the measured data (black points). Graphs (b) and (c) show calculated curves for the permittivity loss along with permittivity loss data (black points). Graph (c) shows the same curves and data as (b), only on an expanded scale to accentuate the data. The black curves in (b) and (c) are the average of the calculated loss curves, while the red curves are 95% confidence curves. The frequency axis is shown on a logarithmic scale. The uncertainties in the measured real-part data were not taken into account. The format of this figure will be followed in the successive figures.

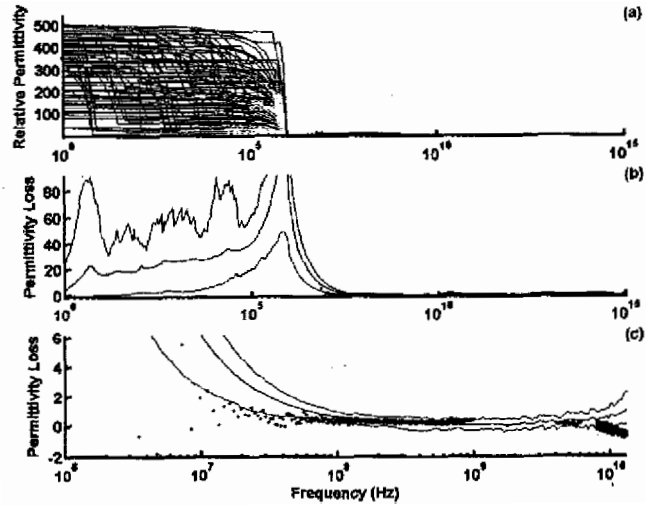

Figure 4. Plots of the real and imaginary parts of the relative permittivity as a function of frequency, overlaid on measured data, with measurement uncertainties in the real part taken into account, for comparison with Figure 3.

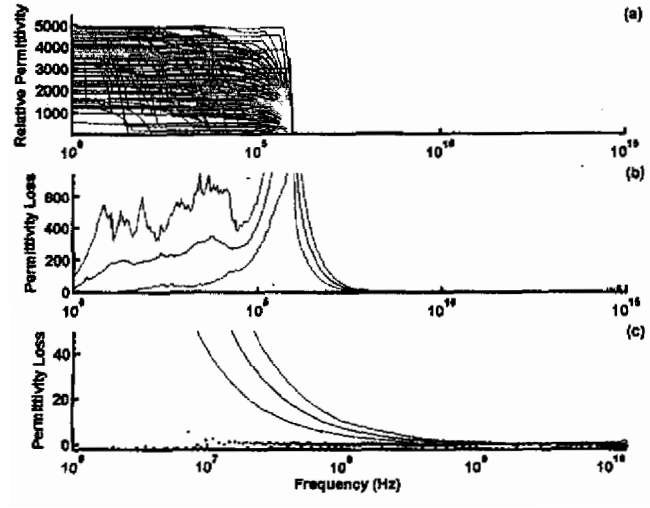

Figure 5. Plots of the real and imaginary parts of the relative permittivity as a function of frequency, overlaid on measured data, with measurement uncertainties in the real part taken into account. For this figure, the maximum-allowed dc permittivity was 5000, in contrast to Figure 4, where the maximum permittivity was 500.

3. A Piecewise-Linear Kramers-Krönig Model

The main drawback of the K-K relations is that they are explicitly true only when one of the two parameters is known over all frequencies. In practice, such knowledge is at least difficult, if not impossible, to obtain. Therefore, in order to use the K-K relations, one must assume and approximate some form of the material's dispersion in the region outside of the known data. If one assumes a real part of the permittivity that is piecewise linear, it is possible to apply working forms of the K-K relations in a rather straightforward manner.

A piecewise-linear model of the permittivity or permeability is a reasonable *approximation* to the behavior of real materials [9, 10]. It should be emphasized here that the real behavior of materials is more complex. Nonetheless, this simple approximation yields much information about materials. Given an increasing sequence of real numbers, $0=\omega_1<\omega_2<\ldots<\omega_{N+1}$, and any sequence of real numbers $a_1,a_2,\ldots,a_N$ with $a_{N+1}=1$, the piecewise-linear model for $\varepsilon_r'(\omega)$ is given by

$$\varepsilon_r'(\omega)=\sum_{n=1}^{N}(A_n\omega+B_n-1)f_n(\omega)+1, \tag{6}$$

where

$$f_n(\omega)=\begin{cases}1, & \omega\in[\omega_n,\omega_{n+1})\\ 0, & \omega\notin[\omega_n,\omega_{n+1})\end{cases} \tag{7}$$

is a square pulse function of width $\omega_{n+1}-\omega_n$. The expressions for A_n and B_n are given by Equations (9) and (10). If such an expression is substituted into Equation (5) and the appropriate integration is performed, a closed-form, singularity-free solution for $\varepsilon_r''(\omega)$ of the form

$$\varepsilon_r''(\omega)=\frac{2}{\pi}A_1L(\omega)+\frac{1}{\pi}\sum_{1}^{N}\Delta A_nL(\Delta\omega)+\frac{1}{\pi}\sum_{1}^{N}(\Delta A_n\omega-\Delta B_n)\ln|\omega_n+\omega_{n+1}| \tag{8}$$

can be obtained. In Equation (8), $\Delta A_n=A_{n+1}-A_n$, $\Delta B_n=B_{n+1}-B_n$, $\Delta\omega_n=\omega-\omega_{n+1}$, and $L(\omega)=\omega\ln\omega$. The parameters A_n, B_n, and ω_n are related to the form of the assumed piecewise-linear real part of the permittivity above, and are given by the relations

$$A_n=\frac{a_{n+1}-a_n}{\omega_{n+1}-\omega_n},\ 1\le n\le N,\ A_{N+1}=0, \tag{9}$$

$$B_n=\frac{a_n\omega_{n+1}-a_{n+1}\omega_n}{\omega_{n+1}-\omega_n},\ 1\le n\le N,\ B_{N+1}=1, \tag{10}$$

where

$$a_{N+1}=1 \tag{11a}$$

and

$$\omega_1=0. \tag{11b}$$

Equations (11) are expressions of the fact that the modeled real part of the relative permittivity is required to go to unity at large frequencies, and that the first frequency value corresponds to a dc applied field.

As an example of this model, consider a real part of the permittivity with $N=9$, which is plotted in Figure 1. In this case, the dimensionless a values and the corresponding frequencies, ω, in rad/s, are as follows: $a_1=a_2=86$, $a_3=a_4=56$, $a_5=a_6=6.5$, $a_7=a_8=1.1$, $a_9=1$, $\omega_1=0$, $\omega_2=16$, $\omega_3=10785$, $\omega_4=1.07\times10^5$, $\omega_5=1\times10^6$, $\omega_6=1.3\times10^{10}$, $\omega_7=1.3\times10^{13}$, $\omega_8=3.1\times10^{14}$, and $\omega_9=4.7\times10^{14}$. These parameters, which are indicative of the magnitude of the real part of the relative permittivity and the corresponding resonant absorption frequencies, are typical of insulating materials [7-9]. Note that the horizontal axis of Figure 1 is shown in a logarithmic scale, which distorts the piecewise linearity of ε_r'.

As is shown in Figure 1, this model generates a real part of the permittivity, ε_r', that is constant at the particular a values over the frequency ranges defined by the corresponding ω_n values. The value of the permittivity is then set to unity from the ω_9 value up to 1×10^{15} rad/s (for the numerical calculations, 1×10^{15} rad/s is taken as infinity). Frequencies higher than 1×10^{15} rad/s create unacceptable levels of numerical noise, due to a limitation in the numerical resolution of the *MatLab*® program. For example, as is shown in the plot of Figure 1, the relative permittivity is equal to 86 from dc up to 16 rad/s, where it then begins to drop linearly until it reaches 56 at 10785 rad/s. It repeats this behavior according to the other parameters listed above, until unity is reached at 4.7×10^{16} rad/s.

Figure 2 shows curves that demonstrate the effect of using Equation (8) in conjunction with the real part of the permittivity

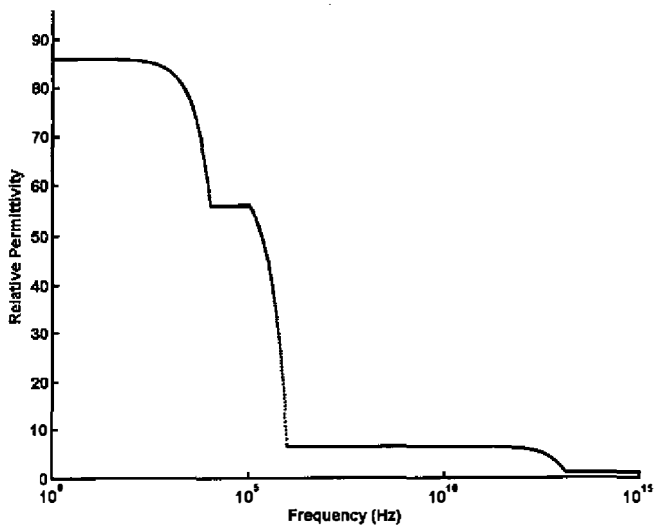

Figure 1. An example plot of the real part of the relative permittivity as a function of frequency according to the piecewise-linear model given by Equation (6). The frequency axis is shown on a logarithmic scale, which distorts the linearity of the generated permittivity.

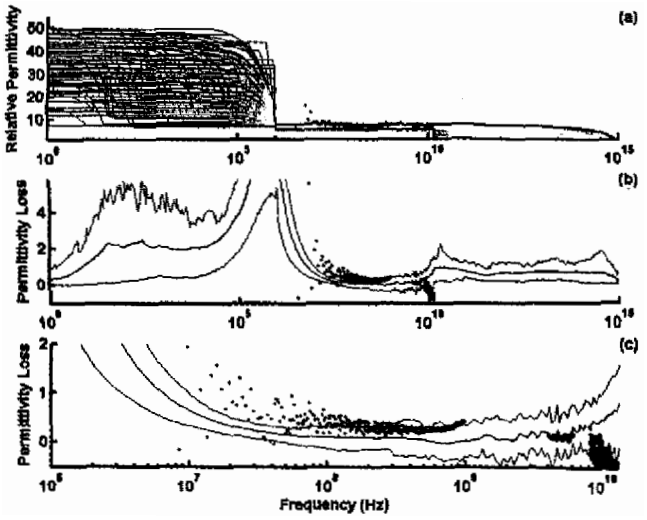

Figure 6. Plots of the real and imaginary parts of the relative permittivity as a function of frequency, overlaid on measured data. These should be considered with Figure 7.

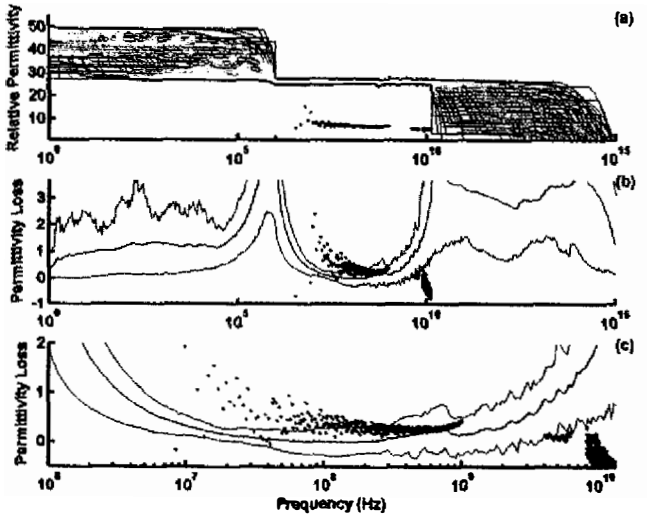

Figure 7. Plots of the real and imaginary parts of the relative permittivity as a function of frequency, overlaid with experimental data. Here, over the measured band of frequencies, the generated real part of the permittivity was arbitrarily raised above the measured data to a value of 26.5. This is in contrast to Figure 6, where the generated real part of the permittivity was required to go through the measured data. When considered with Figure 6, the graphs in this figure demonstrate the lack of influence of the local increase in ε_r' on ε_r''.

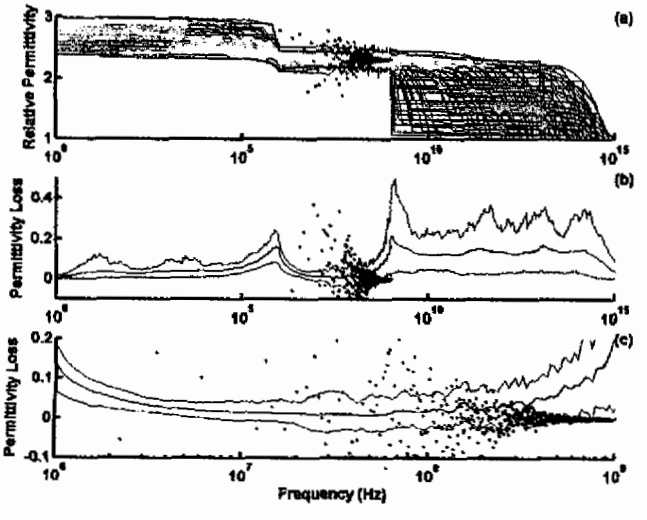

Figure 8. Plots of the real and imaginary parts of the relative permittivity as a function of frequency, overlaid with *low-loss polymer* data.

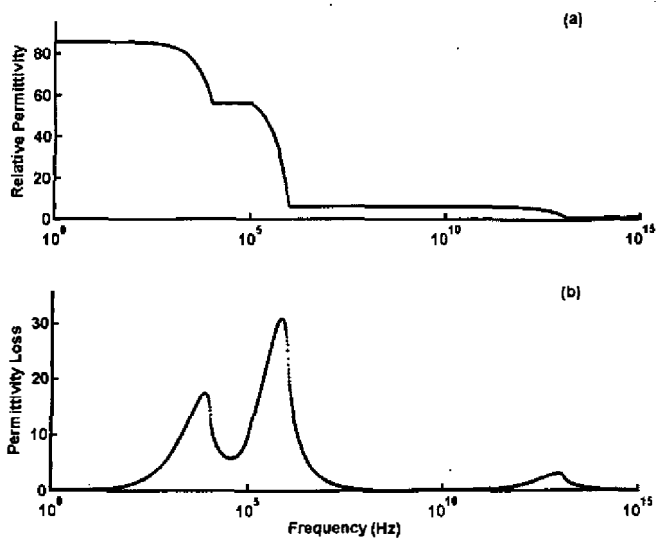

Figure 2. Example plots of the real and imaginary parts of the relative permittivity as a function of frequency. The real part shown in (a) is identical to the real part shown in Figure 1. The imaginary part was calculated using Equation (8) in conjunction with the assumed real part shown in (a). The frequency axis is shown on a logarithmic scale, which creates some distortion to the plots.

shown in Figure 1. Figure 2a reproduces the permittivity, ε_r', shown in Figure 1. Figure 2b shows the imaginary part calculated using the real part in Figure 2a in Equation (8). The following points become evident from an examination of the curves in Figure 2. First, at the positions of the decreases in the real part of the permittivity, the permittivity-loss data show resonances. Additionally, a small or large decrease in the real part of the permittivity corresponds to a small or large value of the loss, respectively. Finally, decreases in the real part that occur over a small or large frequency band yield narrow or broad resonances in the loss, respectively. These observations appear to hold generally, and will be useful when analyzing the data.

4. Measured Data Analysis

Consider now the application of the above model to the analysis of experimental data. In practice, one typically has data over some finite range of frequencies. Additionally, unless measurements are performed near resonance or over a *very* broad range of frequencies, the measured data are flat, within the error of the measurement. If we assume that the real part of the data are well known and of a reliability defined by the standard deviation in the data, the above piecewise-linear K-K model may be used to analyze the loss data over the measured band.

In order to accomplish this goal, the modeled real part of the permittivity is allowed to vary *outside* of the measured frequency band according to the model discussed above. The modeled real part of the permittivity is additionally required to go *through* the experimental data in the measured frequency band. Furthermore, the variation in the modeled real part of the permittivity outside of the measured band is governed by three restrictions. First, the value of the real part of the permittivity must be decreasing – starting from within some chosen maximum dc permittivity – as the frequency increases. Second, the value of the modeled real part of the permittivity at frequencies lower than the measured data may not assume a value lower than the average value of the measured real part of the permittivity. If this were not required, the material would radiate energy when its permittivity increased to the measured value, which is not physically reasonable for the experiments to be considered. Third, the real part of the permittivity must equal unity at and above frequencies of 1×10^{15} rad/s.

If one constructs a large number of realizations for the real part of the permittivity similar to those shown in Figures 1 and 2, then an average of the permittivity loss can be plotted, along with 95% confidence curves. All of this can be overlaid on the data as a means of analysis. For the realizations of the real part of the permittivity below, the pairs of a values were randomly generated with a uniform distribution on a logarithmic scale between the allowed values. In the region below the measured data, the allowed values were between the assumed value of the dc permittivity and the value of the permittivity in the measured band. In the region above the measured data, the allowed values were between the measured permittivity and unity. The ω values were generated according to $\omega = 10^{\beta}$, where β was a randomly generated number.

Figure 3 shows a plot similar in format to Figure 2, with measured real and imaginary permittivity data, along with the modeled (defined and generated) real part and the calculated imaginary part. The measured data were obtained from a composite sample of 40% nickel-zinc ferrite in a silicone-rubber binder. In Figure 3, the maximum value of the dc relative permittivity allowed was 500, and 100 realizations were calculated. In all graphs, the data are shown as black points and appear in a band between 1 MHz and 12 GHz. The red curves in Figure 3a show the 100 different realizations of the real part of the permittivity. In Figures 3b and 3c, which show the permittivity loss, the black curve is the average of all of the calculated loss curves. The red curves in Figures 3b and 3c are 95% confidence bounds. Figure 3c is identical to Figure 3b, but is on an expanded scale, to show only the frequency band of the measured data.

The curves in Figure 3 show, for the assumptions above, which of the measured data points fall within the 95% confidence curves. There are two primary reasons why all the measured data do not all fall within the bounding curves. First, some of the data are clearly bad (as can be seen at the low-frequency end of the measured data, where some of the loss data are negative). Second, the assumptions made about the behavior of the piecewise-linear behavior of the real part of the permittivity may not be sufficient or precise enough to describe the low-frequency behavior of the material (the randomly generated a and ω values may not be representative of the material's behavior). This point will be addressed further, below. It is important to note that the bounding curves did not change position with a larger number of realizations in the real part.

Figure 4 shows the same graphs as Figure 3, except that the uncertainty in the data was taken into account. The standard deviation of the measured data was calculated and used to introduce scatter in each generated realization of the real part of the permittivity. In the region of the measured data, the modeled real part of the permittivity could vary within one standard deviation of the data. The introduction of this scatter caused the bounding curves in Figures 4b and 4c to increase slightly when compared to those

shown in Figure 3. Here, we see that more of the data now lie within the 95% bounding curves.

The calculations above assumed that the maximum value of the dc permittivity was 500. However, it is to be emphasized that how well the *permittivity loss data* in the *microwave* region correspond to the *calculated curves* depends strongly on the *assumed dc* value of the *real part* of the *permittivity*, as well as assumptions made about the general low-frequency behavior of the real part. In order to demonstrate this point, Figure 5 shows the effect of changing the maximum-allowable dc value of the real part of the permittivity compared to the value in Figure 4. The effect was drastic. The graphs in Figure 4 and 5 show that the effectiveness of modeling the data with the K-K relations is strongly dependent on knowledge of the dc permittivity and the general behavior of the permittivity in the unmeasured low-frequency band.

If the dc permittivity was assumed large (Figure 5: maximum-allowed dc permittivity of 5000), the correspondence with the data was poor. If the dc permittivity was assumed relatively small (Figure 4: maximum-allowed dc permittivity of 500), the correspondence with the data was improved. These plots show that some concrete knowledge of the dc permittivity of the material under test is crucial.

Consider now the local behavior of ε_r'' as a function of a corresponding local change in ε_r'. As stated earlier, many band-limited measurements suggest that a larger permittivity at microwave frequencies yielded a larger permittivity loss over that band. Figures 6 and 7 show that *not* to be the case. In Figure 6, the loss curves in Figures 6b and 6c were calculated with the modeled real part of the permittivity in Figure 6a required to go through the measured value of 6.5. Figure 7 shows the same loss calculation with the modeled permittivity forced to go through an arbitrarily higher permittivity of 26.5. In order for the effect to be more visible, the maximum-allowed dc permittivity was chosen to be 50. It is clear from the data in Figures 6c and 7c that the calculated permittivity loss was virtually unaffected by this increase in the microwave permittivity.

One may therefore conclude that the reason the measured data demonstrated an increase in the permittivity loss with the permittivity increase was due to an increase in the *dc* (not microwave) permittivity of the material. This speaks to the primary goal of the investigation. That is, within the framework of this model, there appears to be no principal limit on the permittivity loss with an increase in the permittivity. It appears that increases in the permittivity at low frequencies (or the proximity of the decrease in the permittivity to the microwave band) drive the increase in the permittivity loss.

As a final application, consider the use of the K-K relations as a data analysis tool for low-loss polymers. Figure 8 shows the application of the piecewise-linear K-K model to data on *pure* polyethylene, measured from 1 MHz to 1 GHz. In this case the maximum allowed value of the dc permittivity was chosen to be 3 [1]. The data in Figure 8 show two features of note. First, the experimental data showed typical measurement inaccuracies in ε_r'' for low-loss polymers. Second, the bounding curves could be quite tight when the variation of the dc permittivity was significantly restricted. Such tight bounding curves provide an excellent form of data analysis. Note that the negative values plotted on the lower bounding curve were due to the allowance for scatter in the data. Due to this allowance, the generated real part in the permittivity can have local increases. These increases correspond to negative values of the permittivity loss.

5. Conclusions

The primary conclusions of this K-K work were four-fold. First, the piecewise linear K-K model provides a mechanism for the analysis of confidence, consistency, and error in electromagnetic dispersion data of materials. Second, this analysis revealed much about the general behavior of materials. For example, it was clear from the analysis that low-loss materials fit one of two descriptions. The material must possess either (1) a dc permittivity that is close to its microwave permittivity (low-loss polymers, like Teflon, fit this description); or (2) a large dc permittivity, but experiences a sharp decrease in the permittivity far from microwave frequencies. In these ways, the material either (1) does not absorb energy at or below microwave frequencies, or (2) the resonance absorption occurs far from microwave frequencies and thus does not leak into the microwave region.

Third, the ability to measure the *low-frequency and dc* material characteristics is critical to understanding and analyzing their *microwave* responses. Finally, and most practically, the confidence and error in the material dispersion measurements may, to some degree, be ascertained or improved through use of the K-K relations.

6. References

1. A. von Hippel, *Dielectrics and Waves*, Norwood, MA, Artech House, 1954.

2. H. A. Kramers, *Atti. Cong. Intern. Fisici*, Como, **2**, 1927, p. 545.

3. D. J. Jackson, *Classical Electrodynamics, Third Edition*, New York, John Wiley & Sons, Inc., 1999.

4. L. D. Landau, E. M. Lifshitz, and L. P. Pitaevskii, *Electrodynamics of Continuous Media, Second Edition*, Oxford, Pergamon Press, Ltd., 1984.

5. B. S. Gouray, "Dispersion Relations for Tensor Media and their Application to Ferrites," *J. Appl. Phys.*, **28**, 1957, p. 283.

6. G. W. Milton, D. J. Eyre, and J. V. Mantese, "Finite Frequency Range Kramers Kronig Relations: Bounds on the Dispersion," *Phys. Rev. Lett.*, **79**, 1997, p. 3062.

7. R. C. Hansen, M. Burke, and D. P. Nyquist, "Antennas with Magneto-Dielectrics," *Microwave. Opt. Tech. Lett.*, **26**, 2000, p. 75.

8. G. B. Arfken and H. J. Weber, *Mathematical Methods for Physicists, Fourth Edition*, San Diego, Academic Press, Inc., 1995.

9. Trans-Tech, *Microwave Magnetic and Dielectric Materials: Elements for Microwave Applications*, Adamstown, MD, Trans-Tech, 2004.

10. C. Kittel, *Introduction to Solid State Physics, Sixth Edition*, New York, John Wiley & Sons, Inc., 1986.

11. B. Lax and K. J. Button, *Microwave Ferrites and Ferrimagnetics*, New York, McGraw-Hill Book Company, Inc., 1962.